RSC Advances

PAPER

View Article Online
View Journal | View Issue

Cite this: *RSC Adv.*, 2025, **15**, 34781

Development of a green spectrofluorimetric method for mefenamic acid determination using Rhodamine 6G with mechanistic investigation and central composite design optimization

Arwa Sultan Alqahtani,[a] Maram H. Abduljabbar,[b] Reem M. Alnemari,[c] Saleh I. Alaqel,[d] Ahmed Serag *[e] and Atiah H. Almalki[fg]

Spectrofluorimetry has emerged as a powerful analytical technique offering high sensitivity, selectivity, and environmental compatibility for pharmaceutical analysis. This study aims to develop a novel fluorescence quenching method for mefenamic acid determination using Rhodamine 6G as a molecular probe. Comprehensive spectral characterization revealed that Rhodamine 6G exhibits characteristic absorption at 530 nm and emission at 555 nm, with systematic fluorescence quenching upon mefenamic acid addition while preserving the emission spectral profile. Mechanistic investigation through Stern–Volmer analysis, thermodynamic studies, and Job's method established static quenching *via* 1 : 1 ground-state complex formation with thermodynamic analysis revealing favorable binding driven by electrostatic and π–π interactions. Moreover, central composite design optimization was employed to systematically evaluate pH, Rhodamine 6G concentration, and reaction time, establishing optimal conditions that achieved 76.4% quenching efficiency. Additionally, ICH validation demonstrated excellent analytical performance including linearity over 0.1–4.0 μg mL^{-1} (r^2 = 0.9996), detection limit of 29.2 ng mL^{-1}, accuracy of 98.48%, and precision <2% RSD. Method applications encompassed pharmaceutical formulations with statistical equivalence to reference HPLC methods and human plasma samples with recoveries of 96.30–102.21%. Furthermore, sustainability assessment revealed the superior environmental performance (AGREE score: 0.76 *vs.* 0.66, whiteness: 88.1% *vs.* 72.7%) compared to conventional HPLC methods. This work establishes a practical green alternative for routine mefenamic acid analysis in pharmaceutical quality control and therapeutic monitoring.

Received 4th August 2025
Accepted 15th September 2025

DOI: 10.1039/d5ra05667e

rsc.li/rsc-advances

1. Introduction

Nonsteroidal anti-inflammatory drugs (NSAIDs) represent a cornerstone of modern therapeutic interventions, providing essential anti-inflammatory, analgesic, and antipyretic effects through cyclooxygenase (COX) enzyme inhibition.[1,2] Among this diverse pharmacological class, mefenamic acid exhibits distinctive pharmacological properties that extend beyond conventional COX inhibition mechanisms.[3] This fenamate derivative demonstrates complex molecular interactions, including non-selective COX inhibition with pronounced selectivity toward COX-1 (IC_{50} = 40 nM) over COX-2 (IC_{50} = 3 μM), yielding a 75-fold selectivity ratio.[4] Furthermore, mefenamic acid exhibits significant activity at transient receptor potential melastatin 3 (TRPM3) channels, selectively blocking calcium entry at concentrations of 25–35 μM, which contributes substantially to its analgesic properties.[5] The drug's clinical significance encompasses primary dysmenorrhea management, where 500 mg initial doses followed by 250 mg every six hours demonstrate superior efficacy to the placebo,[6] and menorrhagia treatment, where 500 mg three times daily reduces menstrual blood loss by up to 80%.[7] Additionally, mefenamic acid shows promise in perimenstrual migraine prophylaxis and cancer-related pain management, with efficacy comparable to 650 mg acetaminophen or aspirin.[8] These diverse therapeutic applications, combined with complex pharmacokinetic properties including extensive protein binding (>90%) and dual renal-

[a]*Department of Chemistry, College of Science, Imam Mohammad Ibn Saud Islamic University (IMSIU), P.O. Box 90950, Riyadh 11623, Saudi Arabia*
[b]*Department of Pharmacology and Toxicology, College of Pharmacy, Taif University, P.O. Box 11099, Taif 21944, Saudi Arabia*
[c]*Department of Pharmaceutics and Industrial Pharmacy, College of Pharmacy, Taif University, P.O. Box 11099, Taif 21944, Saudi Arabia*
[d]*Department of Pharmaceutical Chemistry, Faculty of Pharmacy, Northern Border University, Rafha 91911, Saudi Arabia*
[e]*Pharmaceutical Analytical Chemistry Department, Faculty of Pharmacy, Al-Azhar University, Nasr City, Cairo 11751, Egypt. E-mail: Ahmedserag777@hotmail.com*
[f]*Addiction and Neuroscience Research Unit, Health Science Campus, Taif University, P.O. Box 11099, Taif 21944, Saudi Arabia*
[g]*Department of Pharmaceutical Chemistry, College of Pharmacy, Taif University, P.O. Box 11099, Taif 21944, Saudi Arabia*

hepatic elimination pathways, necessitate precise analytical monitoring for therapeutic drug monitoring and pharmaceutical quality control.[9]

A literature survey revealed that high-performance liquid chromatography with ultraviolet detection (HPLC-UV) constitutes the predominant analytical approach for mefenamic acid quantification, with multiple validated methods demonstrating varying analytical performance.[10–13] For example, a stability-indicating method developed by Shah *et al.* utilizing acetonitrile : acetic acid : water (72.5 : 1 : 26.5 v/v/v) mobile phase at pH 3.0 with UV detection at 279 nm achieved linearity from 100–300 μg mL^{-1}, LOD of 10 μg mL^{-1} with a retention time of 3.98 minutes.[10] This approach provides rapid analysis with minimal run time; however, the detection limit remains insufficient for trace-level bioanalytical applications requiring sub-microgram sensitivity. An alternative method by Dhumal *et al.* employed a C8 column with buffer : acetonitrile (55 : 45 v/v) mobile phase at 285 nm detection, demonstrating a retention time of 18.253 minutes and linearity from 0.5–2 μg mL^{-1}.[11] While offering improved sensitivity compared to the previous method, the substantially prolonged analysis time of over 18 minutes per sample limits throughput for routine pharmaceutical analysis. On the other hand, liquid chromatography-tandem mass spectrometry (LC-MS/MS) provides enhanced sensitivity through mass spectrometric detection, addressing sensitivity limitations of UV detection methods. For example, the bioanalytical method developed by Mahadik *et al.* using C18 column with 2 mM ammonium acetate buffer : methanol (15 : 85 v/v, pH 4.5) at 0.75 mL min^{-1} and MRM transitions *m*/*z* 240.0 → 196.3.[14] This method achieved linearity from 20–6000 ng mL^{-1}, LLOQ of 20 ng mL^{-1} and total run time of 1.75 minutes.[14] This method offers high sensitivity and rapid analysis suitable for pharmacokinetic studies; however, the substantial capital investment exceeding $300,000 and specialized technical expertise requirements limit accessibility for routine pharmaceutical laboratories. Electrochemical detection methods were also employed for mefenamic acid determination using modified electrode platforms for enhanced sensitivity with reduced instrumental complexity.[15,16] For example, the method developed by Alagarsamy *et al.* used calcium vanadate nanofilaments/reduced graphene oxide modified glassy carbon electrodes (CVO/RGO/GCE) with differential pulse voltammetry achieving LOD of 0.0079 μM and LOQ of 0.024 μM for biological samples.[15] This approach provides high sensitivity with simple instrumentation; however, electrode preparation requires specialized nanomaterial synthesis protocols and demonstrates susceptibility to fouling in complex matrices. Therefore, there is a clear need for developing rapid, sensitive, and environmentally friendly analytical methods for mefenamic acid determination that overcome these limitations.

Spectrofluorimetry emerges as a powerful alternative analytical technique that addresses many limitations of conventional chromatographic and electrochemical methods while complying with modern analytical chemistry principles of sustainability, cost-effectiveness, and operational simplicity.[17,18] This technique offers inherent advantages including high sensitivity through fluorescence enhancement or quenching mechanisms, excellent selectivity based on specific molecular interactions, reduced instrumentation costs compared to mass spectrometry systems, minimal sample preparation requirements, rapid analysis capabilities, and environmental compatibility.[19,20] Furthermore, spectrofluorimetric methods align with green analytical chemistry principles by minimizing waste generation, reducing energy consumption, and enabling direct analysis in aqueous media, making them particularly attractive for routine pharmaceutical quality control applications and therapeutic drug monitoring.[21–23] Interestingly, few spectrofluorimetric approaches have been developed for mefenamic acid determination. For example, the method developed by Albero *et al.* using aluminum(III) complexation in ethanolic solutions with excitation/emission at λ_{ex} = 355 nm/λ_{em} = 454 nm achieved linear range of 0.30–16.1 μg mL^{-1} with LOD of 0.30 μg mL^{-1}.[24] While offering simplified instrumentation, this approach operates in the blue emission region (454 nm) where biological matrices and pharmaceutical excipients exhibit significant autofluorescence interference, compromising selectivity and accuracy. Another method reported by Tabrizi using cerium(IV) oxidation of mefenamic acid to produce fluorescent cerium(III) with excitation/emission at λ_{ex} = 255 nm/λ_{em} = 354 nm achieved linear range of 0.03–1.5 mg L^{-1} with LOD of 0.009 mg L^{-1}.[25] Although demonstrating acceptable sensitivity, this approach also operates in the UV-blue spectral region where significant matrix interference occurs, requires toxic cerium(IV) reagents, and involves complex oxidation chemistry that may lack selectivity in the presence of other oxidizable pharmaceutical compounds. Recently, a fluorescence quenching method was developed by El Azab *et al.* utilizing *N*-phenyl-1-naphthylamine (NPNA) as fluorescent probe with synchronous fluorescence spectroscopy at 480 nm achieving linearity from 0.50–9.00 μg mL^{-1} and LOD of 60.00 ng mL^{-1}.[26] Despite demonstrating environmental sustainability, this approach suffers from blue region emission interference and limited sensitivity for trace-level biological applications. Among fluorescent probes suitable for pharmaceutical analysis, Rhodamine 6G emerges as a highly promising candidate that addresses the critical autofluorescence limitation while offering superior analytical performance.[27] Rhodamine 6G demonstrates excellent photophysical properties including high quantum yield (0.95 in aqueous solution), strong fluorescence emission in the yellow–green spectral region where biological and pharmaceutical matrices exhibit minimal autofluorescence interference, excellent photostability under ambient conditions, and remarkable sensitivity to molecular interactions.[28] Furthermore, Rhodamine 6G offers superior analytical advantages including cost-effectiveness, water solubility enabling green analytical applications, commercial availability ensuring method reproducibility, and proven analytical performance across diverse matrices.[29]

Therefore, the present study aims to develop and validate a novel, sensitive, and environmentally sustainable "turn-off" fluorescence quenching method for mefenamic acid determination using Rhodamine 6G as the fluorescent probe, addressing the critical analytical gaps identified in current methodologies while adhering to advanced analytical chemistry

principles and green chemistry guidelines. The specific research objectives encompass: (1) comprehensive characterization of the Rhodamine 6G-mefenamic acid interaction mechanism through spectroscopic, thermodynamic, and Stern–Volmer analysis to establish the theoretical basis for analytical method development; (2) systematic optimization of experimental conditions using central composite design (CCD) statistical methodology to achieve maximum analytical performance while minimizing experimental variability; (3) complete method validation following International Conference on Harmonisation (ICH) guidelines including linearity, accuracy, precision, detection limits, quantitation limits, robustness, and selectivity studies; (4) comprehensive application studies encompassing pharmaceutical formulations and biological samples to demonstrate practical analytical utility; and (5) thorough green an sustainability assessment using multiple green analytical chemistry metrics including AGREE,[30] BAGI[31] and whiteness[32] approaches to quantify environmental impact. This work represents the first use of Rhodamine 6G for mefenamic acid analysis, offering a green and cost-effective alternative to existing methods with potential for widespread application in pharmaceutical quality control and therapeutic drug monitoring.

2. Experimental

2.1. Materials and reagents

Mefenamic acid reference standard (purity 99.75%) was generously provided by the Egyptian Drug Authority (EDA, Cairo, Egypt). Rhodamine 6G fluorescent dye (dye content ≥ 95%) was acquired from Sigma-Aldrich (St. Louis, MO, USA). HPLC-grade acetonitrile was also purchased from Sigma-Aldrich (St. Louis, MO, USA). Boric acid, phosphoric acid, acetic acid, sodium hydroxide, and other analytical grade chemicals used for buffer preparation were obtained from El-Nasr Pharmaceutical Chemicals Company (Cairo, Egypt). Commercial mefenamic acid formulations were procured from local community pharmacies in Cairo, Egypt. Freshly prepared distilled water was utilized throughout all experimental procedures. Human plasma samples for method development and validation were kindly supplied by VACSERA Blood Bank (Giza, Egypt), stored at −20 °C until analysis, and thawed at room temperature prior to use.

Mefenamic acid stock solution (100 μg mL^{-1}) was prepared by accurately weighing 10 mg of the reference standard, transferring it to a 100 mL volumetric flask, dissolving in minimal volume of acetonitrile (approximately 10 mL), and diluting to volume with distilled water. Working standard solutions were prepared daily by appropriate serial dilution of the stock solution with distilled water to achieve the required concentrations for calibration and validation studies. Rhodamine 6G stock solution (100 μg mL^{-1}) was prepared by accurately weighing 10 mg of the dye, transferring it to a 100 mL volumetric flask, dissolving completely in distilled water, and diluting to the mark. The solution was stored in an amber glass bottle, protected from light, and remained stable for at least one week when kept at 4 °C. Britton–Robinson buffer solutions covering the pH range 4–8 were prepared by mixing appropriate volumes of a solution containing 0.04 M each of boric acid, phosphoric acid, and acetic acid, followed by precise adjustment to the desired pH using 0.2 M sodium hydroxide solution.

2.2. Instrumentation and software

All fluorescence measurements were performed using a Jasco FP-6200 spectrofluorometer (Jasco International Co., Ltd, Tokyo, Japan) equipped with a 150 W xenon lamp and 1 cm quartz cells. For optimal sensitivity and precision, both excitation and emission bandwidths were set at 5 nm, with the scanning speed maintained at 4000 nm min^{-1}. Spectra Manager software (version 1.53) was utilized for spectral acquisition, data processing, and fluorescence intensity measurements. UV-Vis spectrophotometric studies were conducted using a Shimadzu UV-1800 double-beam spectrophotometer (Shimadzu Corporation, Kyoto, Japan) equipped with 1 cm matched quartz cells and controlled by UV Probe software (version 2.43). The instrument operated with a spectral bandwidth of 1 nm and fast scanning speed across the wavelength range of 220–600 nm. pH measurements and adjustments were precisely monitored using a Jenway 3510 pH meter (Jenway, Staffordshire, UK) calibrated daily with standard buffer solutions (pH 4.0, 7.0, and 10.0) according to manufacturer specifications to ensure accurate pH measurements throughout the experimental work.

Statistical analysis and experimental design optimization were performed using Design Expert® software (version 11.1.2.0, Stat-Ease Inc., Minneapolis, MN, USA) for central composite design implementation, and analysis of variance (ANOVA). Data processing, graphical presentations, and additional statistical calculations were conducted using GraphPad Prism software (version 8.0, GraphPad Software Inc., San Diego, CA, USA). Green analytical chemistry assessment was evaluated using multiple computational tools including AGREE metric calculator and Blue Applicability Grade Index (BAGI) assessment tools both available as software packages, and RGB12 sheet for whiteness sustainability evaluation.

2.3. Optimization of experimental conditions

2.3.1. Scouting phase and risk assessment. Prior to formal experimental design implementation, a comprehensive scouting phase was conducted to identify critical factors affecting the fluorescence quenching efficiency of Rhodamine 6G by mefenamic acid and to assess potential risks that could compromise analytical performance. Initial screening experiments were performed using one-factor-at-a-time (OFAT) approach to evaluate the individual effects of pH (range 3–9), Rhodamine 6G concentration (2–20 μg mL^{-1}), buffer volume (0.2–2.0 mL), reaction time (1–15 minutes), and temperature (15–40 °C) on the fluorescence response. Risk assessment was conducted according to Quality by Design (QbD) principles to identify potential failure modes and their impact on method performance. High-risk factors identified included pH variability affecting both Rhodamine 6G fluorescence properties and complex formation efficiency, and temperature fluctuations

which negatively impact complex formation between the fluorophore and mefenamic acid. Additionally, alkaline pH conditions (>8) were identified as critical risk factors since they promote the conversion of Rhodamine 6G to its non-fluorescent spirolactone form, significantly reducing analytical sensitivity.

2.3.2. Central composite design implementation. Based on scouting results and risk assessment, three critical factors were selected for optimization using central composite design (CCD): pH (X_1), Rhodamine 6G concentration (X_2, μg mL^{-1}), and reaction time (X_3, minutes). The experimental ranges were established as pH 4.0–8.0 to avoid alkaline conditions that promote spirolactone formation, Rhodamine 6G concentration 5.0–15.0 μg mL^{-1}, and reaction time 3.0–10.0 minutes, representing practical analytical conditions while ensuring adequate fluorescence response and method robustness. Temperature was maintained constant at 25 ± 2 °C throughout all experiments to prevent thermal disruption of complex formation. A rotatable CCD with alpha value of 1.2 was employed consisting of 20 experimental runs including 8 factorial points, 6 axial points at distance ±α from the center, and 6 center points for error estimation and lack-of-fit evaluation. The rotatable design ensures uniform prediction variance at all points equidistant from the center, enhancing model reliability across the experimental domain. The design matrix was generated using Design Expert® software with randomized run order to minimize systematic errors and time-related drift effects.

2.3.3. Response variable and model development. The fluorescence quenching efficiency percentage (QE%) was selected as the primary response variable for optimization, calculated using the equation:

$$QE\% = [(F_0 - F)/F_0] \times 100$$

where F_0 represents the fluorescence intensity of Rhodamine 6G alone in the absence of mefenamic acid, and F represents the fluorescence intensity in the presence of mefenamic acid (3.0 μg mL^{-1}). A quadratic polynomial model was then fitted to the experimental data. The adequacy and significance of the developed model were evaluated using analysis of variance (ANOVA) with *F*-test at 95% confidence level ($p < 0.05$). Backward elimination technique was applied to refine the model by removing non-significant terms with *p*-values greater than 0.05, ensuring that only statistically meaningful factors were retained in the final model. Model quality was assessed through coefficient of determination (R^2), adjusted R^2, predicted R^2 values, and adequate precision. Lack-of-fit test was conducted to evaluate model adequacy by comparing pure error variance with lack-of-fit variance, with non-significant lack-of-fit ($p > 0.05$) indicating acceptable model fitting. Following model development and validation, desirability function analysis was employed to determine the optimal experimental conditions that maximize fluorescence quenching efficiency while maintaining practical analytical requirements. The optimized conditions obtained from this analysis were subsequently implemented in the general analytical procedure for method validation and real sample analysis.

2.4. General analytical procedure

The optimized procedure for mefenamic acid determination using Rhodamine 6G as a fluorescent probe was carried out as follows: Into a series of 10 mL volumetric flasks, 1.3 mL of Rhodamine 6G stock solution (100 μg mL^{-1}) and 1.0 mL of Britton–Robinson buffer (pH 6.2) were added and mixed thoroughly. Appropriate volumes of mefenamic acid standard solution or sample solution were then added to achieve final concentrations within the linear range of 0.1–4.0 μg mL^{-1}. The mixtures were gently swirled and allowed to stand for 10.0 minutes at room temperature (25 ± 2 °C) to ensure complete interaction between Rhodamine 6G and mefenamic acid. The solutions were subsequently diluted to the mark with distilled water, and the fluorescence intensities were measured at an emission wavelength of 555 nm after excitation at 526 nm using a 1 cm quartz cell. A blank solution containing all components except mefenamic acid was prepared and its fluorescence intensity (F_0) was measured. The fluorescence intensity (F) of each standard or sample solution was then recorded under identical conditions. A calibration curve was constructed by plotting the mefenamic acid concentration against the ratio (F_0/F). All measurements were performed in triplicate, and mean values were reported.

2.5. Applications to real samples

2.5.1. Analysis of pharmaceutical formulations. For pharmaceutical analysis, commercial mefenamic acid capsules were carefully opened, and the contents were accurately weighed and finely powdered using a mortar and pestle. A quantity of powder equivalent to 25 mg mefenamic acid was transferred to a 250 mL volumetric flask, dissolved in approximately 50 mL distilled water with the aid of sonication for 15 minutes to ensure complete extraction. The solution was filtered through a 0.45 μm membrane filter to remove undissolved excipients, and the filtrate was diluted to volume with distilled water to obtain a stock solution (100 μg mL^{-1}). Working solutions were prepared by appropriate serial dilution with distilled water and analyzed according to the general analytical procedure described in Section 2.4.

2.5.2. Analysis of spiked human plasma samples. Human plasma samples were spiked with mefenamic acid standard solutions to achieve final concentrations of 0.2, 0.5, 1.0, and 3.0 μg mL^{-1} during final analysis. For protein precipitation and sample cleanup, 5 mL of each spiked plasma sample was treated with 15 mL acetonitrile in a 50 mL centrifuge tube, vortexed vigorously for 2 minutes, and centrifuged at 5000 rpm for 10 minutes at 4 °C. The clear supernatant was carefully collected and evaporated to dryness under a gentle stream of nitrogen at 40 °C. The residue was reconstituted with distilled water and vortexed for 30 seconds. For fluorescence analysis, the reconstituted sample was transferred to a 5 mL volumetric flask along with Britton–Robinson buffer (pH 6.2) and Rhodamine 6G solution to achieve final concentrations of 13 μg mL^{-1} Rhodamine 6G, mixed thoroughly, allowed to stand for 10.0 minutes, and diluted to the mark with distilled water. To account for potential matrix effects from plasma components,

matrix-matched calibration curves were constructed using blank plasma processed identically to the samples and spiked with known concentrations of mefenamic acid reference standard.

3. Results and discussion

3.1. Spectral characteristics and photophysical properties

The analytical basis of the developed fluorescence quenching method relies on comprehensive understanding of the spectral behavior and photophysical properties of the Rhodamine 6G-mefenamic acid system. The UV-visible absorption spectra (Fig. 1A) provided critical insight into the individual spectral characteristics and interaction behavior of the analytical components. Rhodamine 6G exhibited a characteristic intense absorption band at 530 nm, attributed to π–π* transitions within the extended xanthene chromophoric system (Fig. 1A). This absorption originates from extensive π-electron delocalization across the tricyclic xanthene framework, where diethylamino substituents at positions 3 and 6 contribute significantly to the bathochromic shift through their strong electron-donating properties. The planar aromatic structure facilitates efficient conjugation between the benzene rings and central pyran moiety, resulting in the characteristic visible region absorption. Mefenamic acid, as a fenamate derivative, demonstrated absorption characteristics typical of substituted benzoic acid derivatives with primary bands around 280 nm and 340 nm, corresponding to π–π* and *n*–π* transitions within the aromatic ring systems and carboxyl group (Fig. 1A). Crucially, mefenamic acid showed negligible absorption beyond 400 nm, indicating minimal direct spectral interference with Rhodamine 6G in the visible region under the described analytical conditions. Upon complex formation, the Rhodamine 6G-mefenamic acid system exhibited distinct spectral modifications compared to the individual components (Fig. 1A). The complex spectrum revealed a notable blue shift from 530 nm to approximately 526 nm, accompanied by a significant hypochromic effect characterized by reduced absorption intensity. These spectral alterations can be attributed to two primary mechanisms: ion-pair formation between cationic Rhodamine 6G and anionic mefenamic acid (deprotonated at pH 6.2) restricts the oscillator strength through electronic coupling, while the close intermolecular association creates an altered electronic environment that reduces the molar absorptivity of Rhodamine 6G compared to its free form. These combined spectral changes provide direct evidence for ground-state complex formation, distinguishing this system from dynamic quenching mechanisms that exhibit no spectral modifications.

The fluorescence characteristics of Rhodamine 6G (Fig. 1B) revealed optimal excitation and emission maxima at 526 nm and 555 nm, respectively, with a Stokes shift of 29 nm. This modest shift indicates minimal structural reorganization between ground and excited states, explaining the exceptionally high fluorescence quantum yield ($\Phi = 0.95$) observed for this

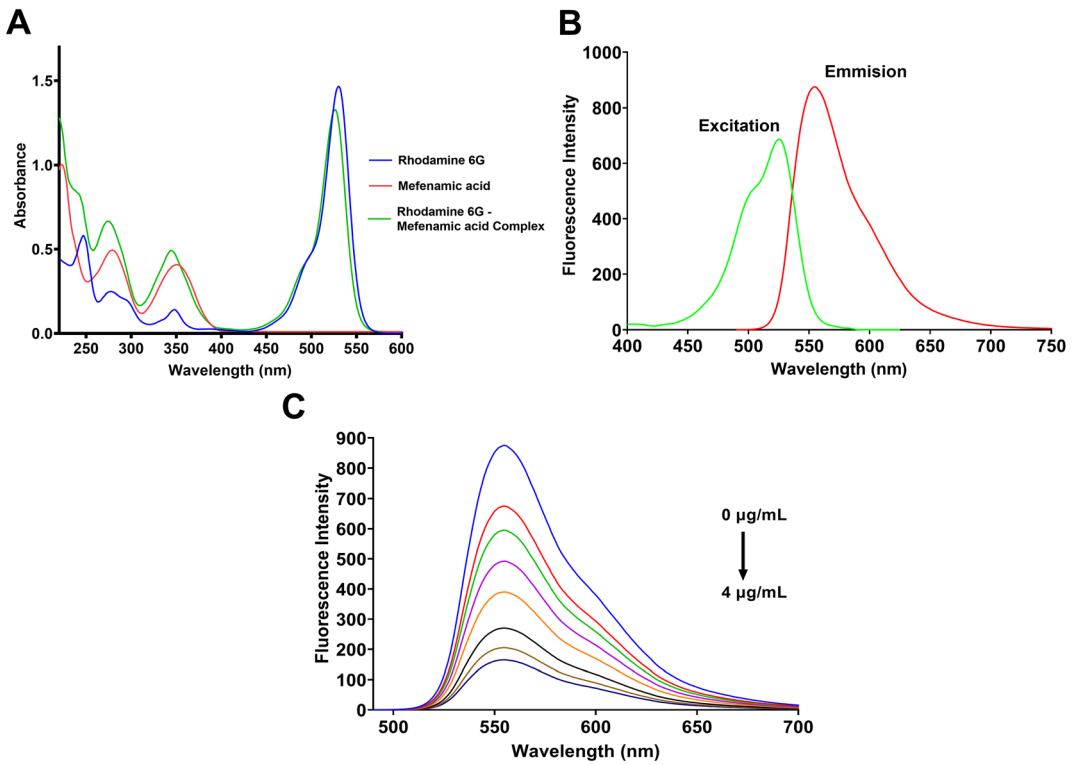

Fig. 1 Spectral characteristics and photophysical properties of the Rhodamine 6G-mefenamic acid system. (A) UV-visible absorption spectra of Rhodamine 6G, mefenamic acid, and Rhodamine 6G-mefenamic acid complex showing blue shift and hypochromic effect upon complex formation. (B) Excitation and emission spectra of Rhodamine 6G showing optimal wavelengths at 526 nm and 555 nm. (C) Concentration-dependent fluorescence quenching of Rhodamine 6G (13 µg mL^{-1}) upon progressive addition of mefenamic acid (0–4.0 µg mL^{-1}) at pH 6.2.

fluorophore. Compared to other xanthene dyes used for pharmaceutical analysis, such as eosin Y and erythrosine B, Rhodamine 6G demonstrates superior photophysical properties with higher quantum yield and enhanced stability in aqueous media.[33,34] Furthermore, the emission wavelength at 555 nm provides excellent analytical advantages, falling within the optimal spectral window that avoids problematic blue region interference (400–480 nm) where biological matrices and pharmaceutical excipients exhibit significant autofluorescence.[35] Concentration-dependent fluorescence measurements (Fig. 1C) demonstrated systematic quenching upon progressive mefenamic acid addition (0–4.0 μg mL^{-1}) while preserving the characteristic emission profile and wavelength maximum. This preservation of spectral shape with proportional intensity decrease indicates homogeneous quenching without significant perturbation of the Rhodamine 6G excited state structure, establishing the basis for quantitative analytical applications.

3.2. Sensing mechanism and thermodynamic studies

The fluorescence quenching mechanism of Rhodamine 6G by mefenamic acid was comprehensively investigated through Stern–Volmer analysis, temperature-dependent studies, and thermodynamic parameter evaluation to establish the fundamental interaction principles governing the analytical method. Initially, the possibility of inner filter effect and Förster resonance energy transfer (FRET) were excluded based on the negligible absorption of mefenamic acid beyond 400 nm (Fig. 1A), ensuring minimal reabsorption of Rhodamine 6G emission at 555 nm. With these mechanisms excluded, Stern–Volmer plots were constructed by plotting F_0/F *versus* mefenamic acid concentration at three different temperatures (298 K, 303 K, and 313 K) to differentiate between static and dynamic quenching mechanisms (Fig. 2A). The linear Stern–Volmer relationships observed at all temperatures followed the classical equation $F_0/F = 1 + K_{sv}[Q]$, where K_{sv} represents the Stern–Volmer quenching constant and $[Q]$ is the quencher concentration. The calculated Stern–Volmer constants decreased systematically with increasing temperature from 2.43×10^5 M^{-1} at 298 K to 2.18×10^5 M^{-1} at 303 K and 1.76×10^5 M^{-1} at 313 K (Table 1), demonstrating an inverse temperature dependence characteristic of static quenching mechanisms. This temperature behavior definitively excludes dynamic quenching, where K_{sv} values typically increase with temperature due to enhanced molecular motion and collision frequency. Importantly, these values are significantly higher than those reported for other fluorescence-based drug analysis systems, such as the eosin Y-linagliptin system,[36] indicating superior binding affinity and enhanced analytical sensitivity. The association constants (K_a)

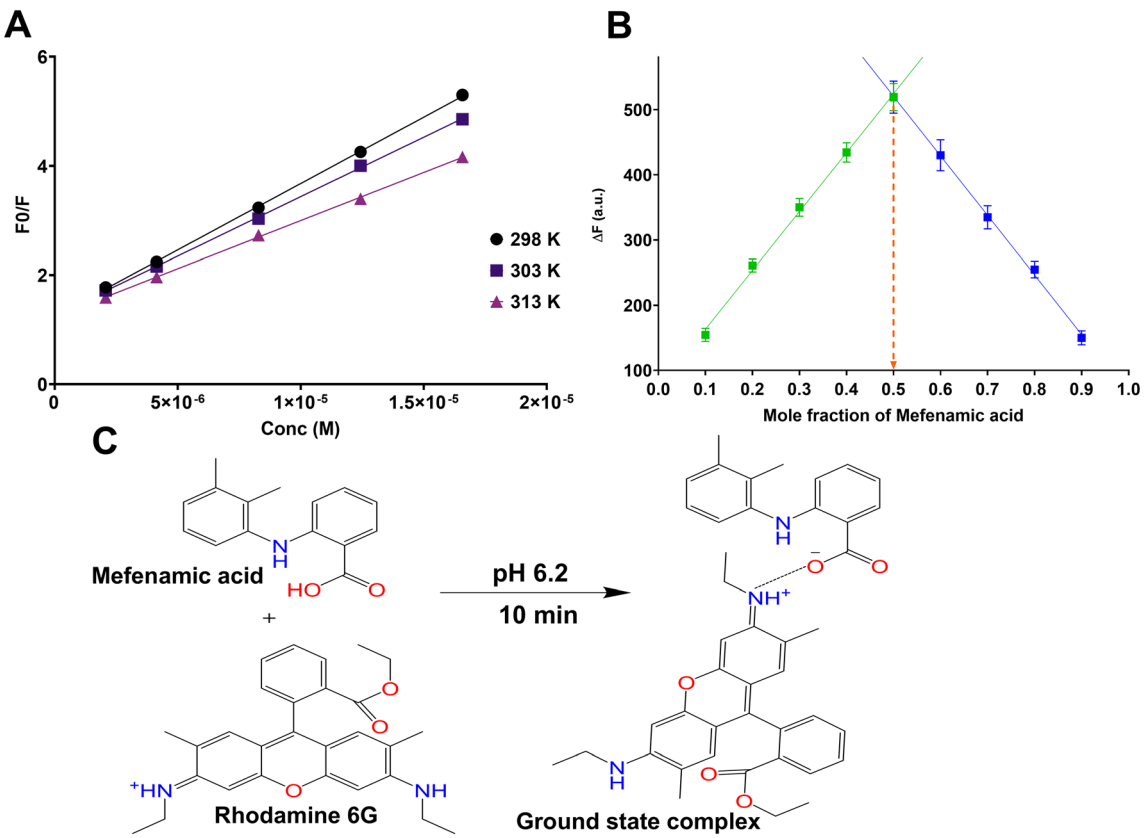

Fig. 2 Sensing mechanism and thermodynamic characterization. (A) Stern–Volmer plots at different temperatures (298 K, 303 K, 313 K) showing linear relationships with decreasing slopes confirming static quenching mechanism. (B) Job's method plot demonstrating 1 : 1 binding stoichiometry with maximum at 0.5 mole fraction of mefenamic acid. (C) Proposed interaction mechanism showing ground-state complex formation between cationic Rhodamine 6G and anionic mefenamic acid through electrostatic interaction.

Table 1 Thermodynamic parameters for Rhodamine 6G-mefenamic acid interaction at different temperatures

Temperature (K)	K_{sv} (10^5 M^{-1})	K_a (10^5 M^{-1})	ΔG (kJ mol^{-1})	ΔH (kJ mol^{-1})	ΔS (J (mol^{-1} K^{-1}))
298	2.43	4.04	−32.00	−13.87	60.81
303	2.18	3.78	−32.37		
313	1.76	3.09	−32.91		

were subsequently calculated using the modified Stern–Volmer equation for static quenching systems, yielding values of 4.04×10^5 M^{-1} at 298 K, 3.78×10^5 M^{-1} at 303 K, and 3.09×10^5 M^{-1} at 313 K (Table 1), which followed the same inverse temperature dependence pattern as the K_{sv} values.

Thermodynamic parameters were then calculated from the temperature dependence of K_a to elucidate the driving forces governing complex formation (Table 1). The Gibbs free energy changes (ΔG) were calculated using the equation $\Delta G = -RT \ln K_a$, yielding values of −32.00, −32.37, and −32.91 kJ mol^{-1} at 298, 303, and 313 K, respectively. The negative ΔG values confirm thermodynamically favorable spontaneous complex formation at all temperatures studied. The enthalpy change (ΔH = −13.87 kJ mol^{-1}) and entropy change (ΔS = 60.81 J (mol^{-1} K^{-1})) were determined from van't Hoff plot analysis using the relationship $\ln K_a = -\Delta H/RT + \Delta S/R$. The negative enthalpy indicates exothermic binding driven by favorable intermolecular interactions, while the positive entropy suggests increased disorder upon complex formation, likely due to desolvation of the binding partners and release of structured water molecules. These thermodynamic parameters are consistent with electrostatic binding mechanisms reported for similar fluorophore-drug interactions, such as those observed for erythrosine B-raloxifene system[21] and terbium-doped carbon quantum dots-alogliptin system,[37] confirming the proposed ion-pair formation mechanism.

The stoichiometry of the Rhodamine 6G-mefenamic acid complex was determined using Job's method of continuous variation (Fig. 2B). The Job plot, constructed by plotting the change in fluorescence intensity (ΔF) *versus* the mole fraction of mefenamic acid while maintaining constant total concentration of 1×10^{-5} M, exhibited a maximum at mole fraction 0.5, confirming a 1 : 1 binding stoichiometry between Rhodamine 6G and mefenamic acid. This result indicates formation of a well-defined binary complex with equimolar binding ratio, supporting the proposed ground-state association mechanism. The symmetrical bell-shaped curve with a clear maximum at 0.5 mole fraction demonstrates strong binding affinity and excludes the possibility of higher-order complex formation under the experimental conditions.

The proposed interaction mechanism (Fig. 2C) involves ground-state complex formation between cationic Rhodamine 6G and mefenamic acid through multiple complementary interactions. At the working pH of 6.2, mefenamic acid exists predominantly in its anionic form ($pK_a = 4.2$), enabling strong electrostatic interactions with the positively charged xanthene ring system of Rhodamine 6G. Additionally, π–π stacking interactions could occur between the aromatic systems, facilitated by the planar conformations of both molecules. This multi-point recognition mechanism explains the high binding affinity and selectivity observed, while the resulting ground-state complex exhibits reduced fluorescence efficiency due to altered electronic properties and restricted conformational freedom of the Rhodamine 6G chromophore. The formation of this stable 1 : 1 complex serves as the fundamental basis for the quantitative determination of mefenamic acid through proportional fluorescence quenching.

3.3. Statistical optimization using central composite design

The analytical performance of the Rhodamine 6G-based fluorescence quenching method was systematically optimized using central composite design (CCD) to achieve maximum quenching efficiency while ensuring robust analytical conditions. Following comprehensive scouting studies and risk assessment, three critical factors were identified for optimization: pH (A), Rhodamine 6G concentration (B), and reaction time (C). The experimental design encompassed 20 runs including factorial points, axial points, and center points to evaluate main effects, interactions, and quadratic terms (Table S1). The fluorescence quenching efficiency (QE%) served as the response variable. This systematic approach enabled comprehensive evaluation of factor effects and their interactions while minimizing the number of experiments required for optimization.

Analysis of variance (ANOVA) was performed to evaluate model significance, adequacy, and individual factor contributions (Table 2). The developed reduced quadratic model demonstrated high statistical significance with an F-value of 165.45 and $p < 0.0001$, confirming that the model effectively explains the experimental variance. The model's high significance indicates that the probability of such a large F-value occurring due to noise is less than 0.01%. Individual factor analysis revealed that all main effects were statistically significant ($p < 0.0001$), with A-pH ($F = 141.02$) and B-reagent concentration ($F = 146.97$) showing the strongest influences on quenching efficiency, while C-Reaction time ($F = 40.28$) demonstrated moderate but significant impact. The interaction terms AB ($F = 155.78$) and BC ($F = 13.79$) were both significant, indicating synergistic effects between pH and reagent concentration, and between reagent concentration and reaction time. The quadratic terms A^2 ($F = 298.48$) and B^2 ($F = 147.75$) showed high significance, confirming substantial curvature in the response surface and validating the quadratic model selection. The lack of fit test yielded $F = 3.23$ with $p = 0.1078$ (not significant), indicating adequate model fitting without systematic deviation from experimental data.

Table 2 Analysis of variance (ANOVA) results for central composite design optimization

Source	Sum of squares	d*f*	Mean square	*F*-value	*p*-value	
Model	6899.34	7	985.62	165.45	< 0.0001	Significant
A-pH	840.10	1	840.10	141.02	< 0.0001	
B-reagent conc.	875.53	1	875.53	146.97	< 0.0001	
C-reaction time	239.93	1	239.93	40.28	< 0.0001	
AB	928.02	1	928.02	155.78	< 0.0001	
BC	82.17	1	82.17	13.79	0.0030	
A^2	1778.11	1	1778.11	298.48	< 0.0001	
B^2	880.19	1	880.19	147.75	< 0.0001	
Residual	71.49	12	5.96			
Lack of fit	58.53	7	8.36	3.23	0.1078	Not significant
Pure error	12.96	5	2.59			
Cor total	6970.83	19				

The final empirical model in coded factors was established as:

$$\mathrm{QE\%} = +67.92 + 8.79A + 8.97B + 4.70C + 10.77AB + 3.20BC - 17.93A^2 - 12.61B^2$$

Analysis of coefficient magnitudes and signs provides valuable insights into factor influences and their practical implications. The positive linear coefficients for all factors (*A*: +8.79, *B*: +8.97, *C*: +4.70) indicate that increasing pH, reagent concentration, and reaction time within the experimental range generally enhance quenching efficiency. The similar magnitudes of pH and reagent concentration coefficients (8.79 *vs.* 8.97) confirm their comparable importance, while the smaller reaction time coefficient (4.70) reflects its more moderate influence. The substantial positive interaction coefficient AB (+10.77) demonstrates strong synergistic effects between pH and reagent concentration, suggesting that optimal performance requires simultaneous optimization of both factors. The negative quadratic coefficients (A^2: −17.93, B^2: −12.61) indicate curvature with well-defined maxima for both pH and reagent concentration, confirming the existence of optimal values rather than monotonic relationships. The larger magnitude of the A^2 coefficient suggests that pH optimization is more critical than reagent concentration optimization. Model validation was conducted through comprehensive analysis (Table S2 and Fig. S1), demonstrating excellent statistical parameters with $R^2 = 0.9897$, adjusted $R^2 = 0.9838$, and predicted $R^2 = 0.9607$. The adequate precision of 35.58 exceeded the minimum threshold of 4, confirming excellent signal-to-noise ratio. Diagnostic plots showed normal distribution without systematic patterns, validating model adequacy and reliability (Fig. S1).

The individual factor effects and their interactions were systematically evaluated through response surface methodology and directly correlated with ANOVA findings (Fig. 3 and 4). The pH effect (Fig. 3A) demonstrated a distinct parabolic relationship with maximum quenching efficiency around pH 6.2, directly reflecting the significant *A* and A^2 terms in the ANOVA table. This behavior confirms the complex interplay between Rhodamine 6G fluorescence stability and mefenamic acid ionization state. At lower pH values (<5), reduced quenching efficiency resulted from incomplete deprotonation of mefenamic acid ($pK_a = 4.2$), limiting electrostatic interactions with cationic Rhodamine 6G. Conversely, at higher pH values (>7), decreased efficiency occurred due to potential Rhodamine 6G structural changes and reduced complex stability. The Rhodamine 6G concentration effect (Fig. 3B) revealed an optimal concentration around 12.6 μg mL^{-1}, consistent with the significant *B* and B^2 terms, where maximum fluorescence signal and analytical sensitivity were achieved. Below this concentration, insufficient fluorescence intensity limited detection capability, while higher concentrations led to self-quenching phenomena. The reaction time investigation (Fig. 3C) showed gradual increase in quenching efficiency reaching equilibrium around 10 minutes, reflecting the moderate but significant *C* term and indicating complete complex formation kinetics. The interaction effects were thoroughly visualized through interaction plots and 3D response surfaces (Fig. 4). The pH-reagent concentration interaction (Fig. 4A and B) clearly demonstrated the synergistic effects predicted by the highly significant AB term, where optimal performance required simultaneous optimization of both factors. The 3D response surface (Fig. 4B) showed a well-defined maximum region, confirming the existence of optimal conditions within the experimental domain. The reagent concentration-reaction time interaction (Fig. 4C and D) displayed the moderate interaction effects corresponding to the significant BC term, indicating that longer reaction times were particularly beneficial at intermediate reagent concentrations.

Desirability function optimization was employed to determine the optimal experimental conditions that maximize quenching efficiency while maintaining practical analytical requirements (Fig. S2). The numerical optimization procedure, incorporating the validated quadratic model, identified optimal conditions as pH 6.19, Rhodamine 6G concentration 12.6 μg mL^{-1}, and reaction time 9.96 minutes, yielding a predicted quenching efficiency of 76.6% with overall desirability of 1.0. For practical analytical implementation, these conditions were rounded to pH 6.2, Rhodamine 6G concentration 13.0 μg mL^{-1}, and reaction time 10.0 minutes, which maintained the predicted high quenching efficiency while ensuring ease of

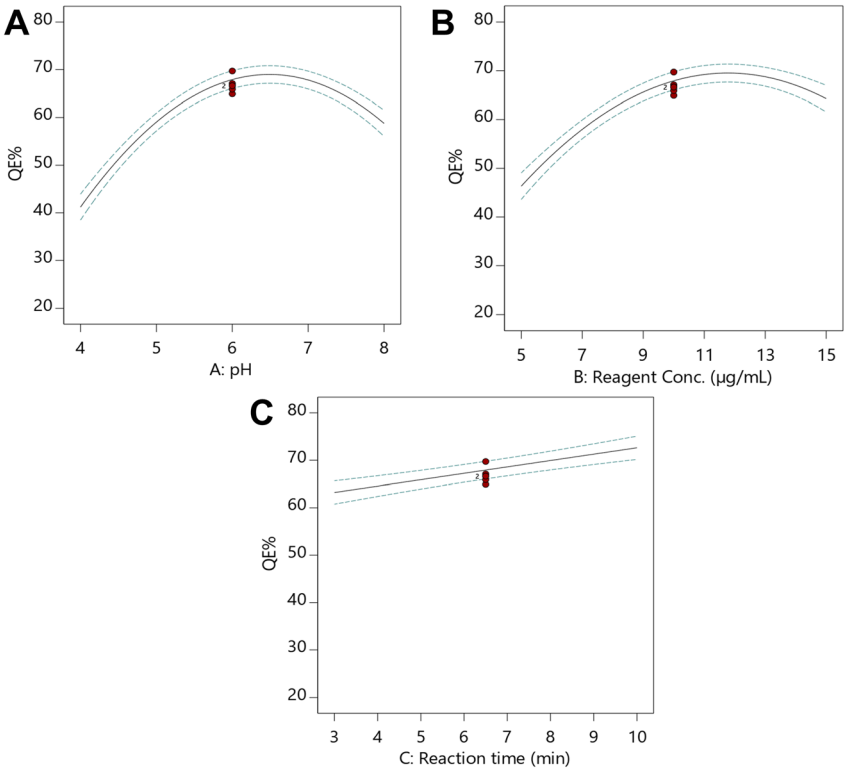

Fig. 3 Individual factor effects from central composite design optimization. (A) Effect of pH on quenching efficiency showing optimal response around pH 6.2. (B) Effect of Rhodamine 6G concentration demonstrating maximum efficiency at approximately 12.6 µg mL^{-1}. (C) Effect of reaction time (factor C) displaying a linear increase in quenching efficiency with equilibrium around 10 minutes, confirming progressive complex formation kinetics. Red dots represent center points of the experimental design, with confidence intervals shown as dashed lines.

preparation and reproducibility in routine laboratory operations. These conditions represent the global optimum within the experimental domain, balancing maximum analytical performance with practical considerations such as reagent consumption and analysis time. The design space analysis (Fig. S3) revealed the operational region where quenching efficiency exceeds 70%, providing robust conditions for routine analytical applications. The optimized conditions derived from this comprehensive statistical approach were subsequently implemented in all validation studies and real sample analyses, providing the basis for reliable, reproducible, and high-performance analytical methodology suitable for pharmaceutical quality control and therapeutic drug monitoring applications.

3.4. Method validation according to ICH guidelines

The developed Rhodamine 6G-based fluorescence quenching method was comprehensively validated following ICH Q2(R2) guidelines to ensure reliability, accuracy, and precision for pharmaceutical analysis.[38]

Linearity studies were conducted over the concentration range of 0.1–4.0 µg mL^{-1} using freshly prepared standard solutions analyzed in triplicate (Table 3). The calibration curve, constructed by plotting the fluorescence intensity ratio (F_0/F) *versus* mefenamic acid concentration, demonstrated excellent linearity with a correlation coefficient (r^2) of 0.9996. The linear regression equation was established as $F_0/F = 1.0113C + 1.2370$, where C represents the mefenamic acid concentration in µg mL^{-1}. The slope value of 1.0113 indicates high sensitivity, while the y-intercept of 1.2370 reflects minimal systematic error. The excellent correlation coefficient confirms strong linear relationship between response and concentration across the entire analytical range. Detection and quantitation limits were determined using signal-to-noise ratio approach based on the standard deviation of the blank and slope of the calibration curve. The limit of detection (LOD) was calculated as 29.2 ng mL^{-1}, while the limit of quantitation (LOQ) was 96.4 ng mL^{-1} (Table 3). These values demonstrate high sensitivity, significantly lower than therapeutic plasma concentrations of mefenamic acid, ensuring adequate sensitivity for both pharmaceutical quality control and bioanalytical applications. The low detection limits highlight the superior analytical performance compared to conventional UV-based HPLC methods, which typically achieve LOD values in the microgram range.

Accuracy and precision studies were conducted at three concentration levels within the linear range (Table 3). Accuracy, expressed as percentage recovery, averaged 98.48 ± 1.47%, demonstrating excellent agreement between measured and true values with minimal systematic bias. Repeatability precision (intra-day precision) was evaluated through nine determinations (three concentrations analyzed

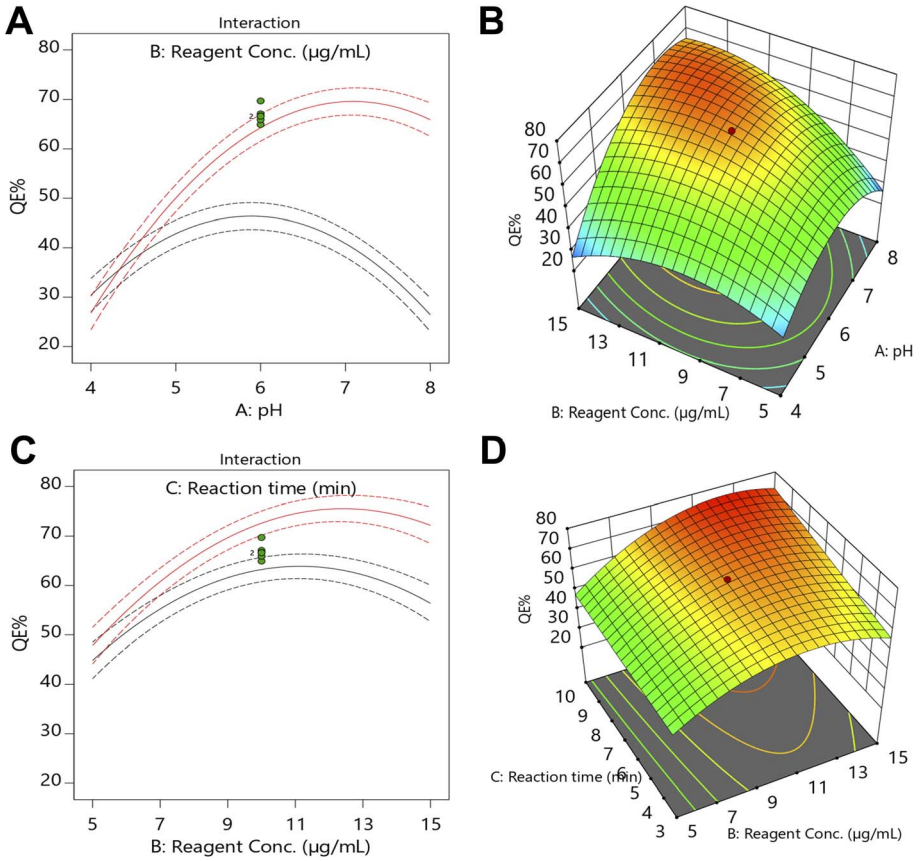

Fig. 4 Interaction effects and response surface analysis from central composite design showing synergistic factor relationships and three-dimensional response optimization. (A) pH-Rhodamine 6G concentration interaction plot demonstrating strong synergistic effects with optimal performance requiring simultaneous optimization of both factors. (B) Three-dimensional response surface plot for pH and Rhodamine 6G concentration where different colors represent quenching efficiency levels: green indicates lower QE% values, yellow represents intermediate values, and red/orange shows the maximum QE% region (optimal conditions), confirming the existence of optimal conditions within the experimental domain. (C) Rhodamine 6G concentration-reaction time interaction plot indicating moderate interaction effects, where longer reaction times are particularly beneficial at intermediate reagent concentrations. (D) Three-dimensional response surface plot for Rhodamine 6G concentration and reaction time illustrating the combined effect of these factors on quenching efficiency.

Table 3 Method validation parameters according to ICH Q2(R2) guidelines

Parameters		Mefenamic acid
Excitation wavelength (nm)		526
Emission wavelength (nm)		555
Linearity range (µg mL^{-1})		0.1–4.0
Slope		1.0113
Intercept		1.2370
Correlation coefficient (r^2)		0.9996
LOD (ng mL^{-1})		29.223
LOQ (ng mL^{-1})		96.435
Accuracy[a] (% R)		98.48 ± 1.472
Repeatability precision[b] (% RSD)		1.495
Intermediate precision[c] (% RSD)		1.892
Robustness (%R)	pH	98.40 ± 0.953
	Reagent conc.	99.77 ± 1.134
	Reaction time	101.78 ± 1.184

[a] Average of 9 determinations (3 concentrations repeated 3 times). [b] % RSD of 9 determinations (3 concentrations repeated 3 times) measured on the same day. [c] % RSD of 9 determinations (3 concentrations repeated 3 times) measured in the three consecutive days.

in triplicate on the same day), yielding a relative standard deviation (RSD) of 1.50%. Intermediate precision (inter-day precision) was assessed through nine determinations performed over three consecutive days, resulting in an RSD of 1.89%. Both precision parameters were well below the acceptable limit for analytical methods, demonstrating excellent method reproducibility and reliability. Robustness evaluation was conducted by deliberately varying critical method parameters within realistic ranges to assess method resilience to minor operational changes (Table 3). The investigated parameters included pH (6.2 ± 0.2), Rhodamine 6G concentration (13.0 ± 1.0 µg mL^{-1}), and reaction time (10.0 ± 1.0 minutes). Recovery percentages remained within acceptable limits for all tested variations: pH variation yielded 98.40 ± 0.95% recovery, reagent concentration variation achieved 99.77 ± 1.13% recovery, and reaction time variation resulted in 101.78 ± 1.18% recovery. The low RSD values (all <1.2%) demonstrate that minor variations in experimental conditions do not significantly affect analytical performance, confirming method robustness suitable for routine analytical applications.

Selectivity studies were performed to evaluate potential interference from common pharmaceutical excipients, ions, and biological matrix components (Fig. 5). The fluorescence quenching response was assessed in the presence of various potential interferents at concentrations typically encountered in pharmaceutical formulations and biological samples. Mefenamic acid demonstrated the highest quenching efficiency, significantly higher than all tested interferents. Common pharmaceutical excipients including starch, lactose, magnesium stearate, cellulose, and sodium lauryl sulfate showed minimal interference (QE% < 5%), confirming excellent selectivity. Inorganic ions frequently present in biological matrices (Na^+, K^+, Ca^{2+}, Mg^{2+}, Cl^-, SO_4^{2-}, PO_4^{3-}) exhibited negligible quenching effects (<4%). Metabolites including tryptophan, tyrosine, glutamic acid, glucose, and pooled plasma showed also minimal interference (<5%), demonstrating excellent selectivity for mefenamic acid determination. The substantial difference between mefenamic acid response and potential interferents (10-fold higher) provides adequate analytical specificity for accurate quantitation in the presence of matrix components.

However, it should be acknowledged that the current selectivity assessment has inherent limitations characteristic of fluorescent probe-based methods. Other structurally related drugs containing similar functional groups, particularly carboxylic acid moieties and aromatic amine substituents, could potentially interact with Rhodamine 6G through comparable binding mechanisms. This non-selective binding represents a fundamental disadvantage of fluorescent probes, where molecular recognition relies primarily on general electrostatic and π–π stacking interactions rather than highly specific molecular complementarity. For applications requiring enhanced selectivity, particularly in complex biological matrices containing multiple drug compounds, improved selectivity could be achieved through integration with molecularly imprinted polymers (MIPs).[39] MIP-based separation prior to fluorescence detection would provide highly specific molecular recognition cavities complementary to mefenamic acid structure, effectively eliminating potential interference from structurally similar compounds while maintaining the sensitivity advantages of the fluorescence detection system.

Nevertheless, the developed method offers significant practical advantages that often outweigh these selectivity limitations in routine pharmaceutical analysis. The method's cost-effectiveness, requiring only standard fluorescence instrumentation and inexpensive reagents, makes it highly accessible for resource-limited laboratories. The simplicity of the analytical procedure, involving minimal sample preparation and straightforward fluorescence measurements, enables rapid implementation without extensive operator training or specialized expertise. Furthermore, the comprehensive validation results demonstrate that the developed Rhodamine 6G-based fluorescence quenching method meets all ICH Q2(R2) requirements for analytical method validation. The combination of excellent linearity, high sensitivity, superior accuracy and precision, robust performance, and exceptional selectivity establishes the method's suitability for reliable quantitative determination of mefenamic acid in pharmaceutical and biological samples.

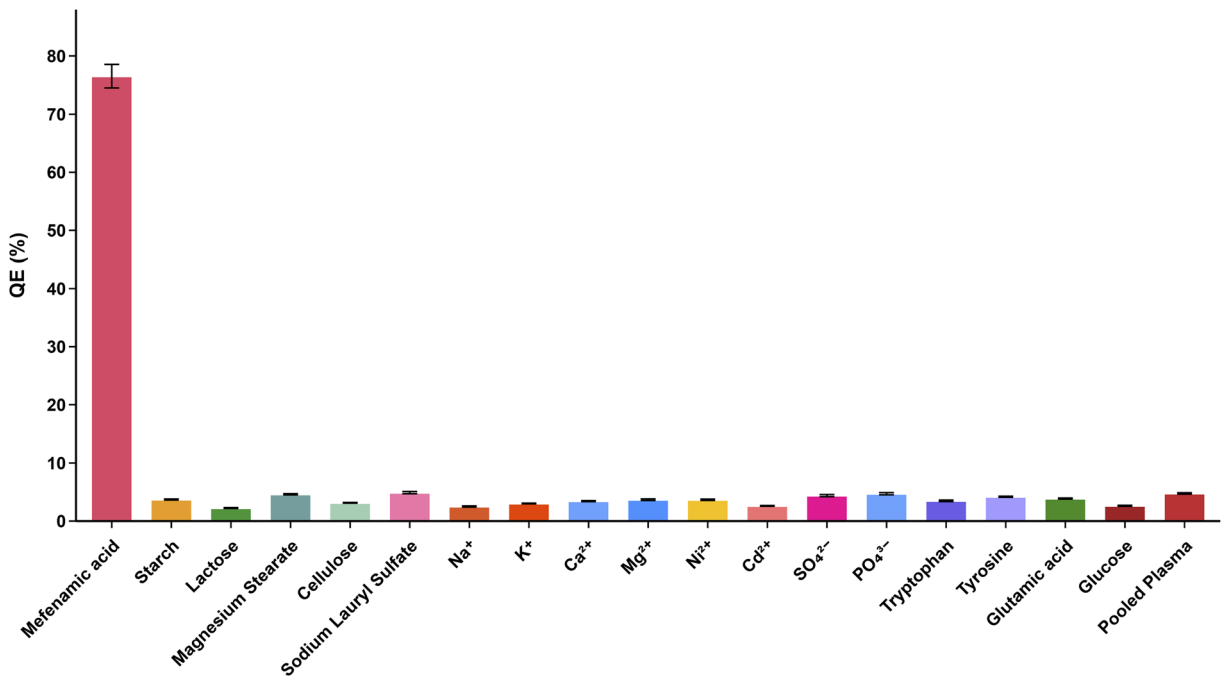

Fig. 5 Selectivity study showing fluorescence quenching efficiency (QE%) of mefenamic acid compared to potential interferents including pharmaceutical excipients, inorganic ions, and biological matrix components. Mefenamic acid demonstrates significantly higher quenching efficiency than all tested interferents.

3.5. Method application studies

The practical utility and analytical performance of the developed Rhodamine 6G-based fluorescence quenching method were demonstrated through comprehensive application studies encompassing pharmaceutical formulations and plasma samples.

Commercial mefenamic acid capsules (250 mg) were analyzed using the developed fluorescence method and results were statistically compared with the established HPLC-UV method[10] (Table 4). The fluorescence method yielded mean recovery of 99.94 ± 0.871%, demonstrating excellent accuracy for pharmaceutical quality control applications. Statistical evaluation using Student's *t*-test showed no significant difference between the developed method and the reported HPLC method (*t*-calculated = 0.336, *t*-critical = 2.306 at $p = 0.05$), confirming analytical equivalence. *F*-test analysis for precision comparison yielded *F*-calculated = 1.582 (*F*-critical = 6.338), demonstrating comparable precision between methods. The bias analysis using θ_L and θ_U values (−1.233 and 1.653, respectively) fell within the acceptable ±2% range, confirming that the developed method meets pharmaceutical analysis requirements. These results establish the fluorescence method as a reliable alternative to conventional HPLC analysis for routine pharmaceutical quality control, offering superior analytical throughput and reduced operational costs while maintaining equivalent analytical performance.

The method's applicability to biological samples was evaluated through comprehensive analysis of spiked human plasma samples at clinically relevant concentration levels (Table S3). Clinical pharmacokinetic studies in preterm infants demonstrate significant inter-individual variation in mefenamic acid plasma concentrations following 2 mg kg^{-1} oral administration. Peak plasma concentrations (C_{max}) varied from 1.2 to 6.1 μg mL^{-1} with a mean of 3.8 μg mL^{-1}, while time to reach C_{max} (t_{max}) ranged from 2 to 18 hours with a mean of 7.7 hours.[40] Importantly, therapeutic efficacy appears concentration-dependent, with plasma concentrations required to be above 2.0 μg mL^{-1} and maintained for at least 12 hours for effective ductus closure in preterm infants. The substantial inter-individual pharmacokinetic variation (C_{max} range: 1.2–6.1 μg mL^{-1}) and the critical therapeutic threshold of 2.0 μg mL^{-1} highlight the importance of accurate bioanalytical methods for therapeutic drug monitoring applications.

To encompass the clinically relevant concentration range while addressing potential sub-therapeutic monitoring needs, plasma samples were spiked at four concentration levels: 0.2, 0.5, 1.0, and 3.0 μg mL^{-1}. These concentrations represent the lower range of therapeutic monitoring, accounting for potential drug metabolism, protein binding effects, and the need for sensitive bioanalytical methods capable of detecting mefenamic acid at concentrations below peak therapeutic levels. Recovery studies demonstrated excellent analytical performance across all tested concentration levels (Table S3). At the lowest spiked concentration (0.2 μg mL^{-1}), the method achieved 99.56% recovery with 3.42% RSD ($n = 3$), confirming adequate sensitivity for trace-level determinations below typical therapeutic concentrations. Mid-range concentrations of 0.5 and 1.0 μg mL^{-1} yielded recoveries of 102.21% (3.14% RSD) and 96.30% (2.12% RSD), respectively, demonstrating consistent performance across the therapeutic monitoring range. At the highest tested concentration (3.0 μg mL^{-1}), recovery was 98.35% with 1.72% RSD, showing improved precision at higher analyte levels. All recovery values fell within the acceptable range for bioanalytical methods, while precision values were well below the 15% limit typically required for biological sample analysis. The systematic decrease in RSD values with increasing concentration (3.42% to 1.72%) reflects improved signal-to-noise ratios at higher analyte levels, consistent with the method's detection limits and linear range. The excellent recovery and precision data, encompassing concentrations relevant to therapeutic drug monitoring applications, establish the developed method as a viable analytical tool for mefenamic acid determination in biological matrices, offering significant advantages in terms of analysis time, cost-effectiveness, and operational simplicity compared to conventional LC-MS/MS bioanalytical methods while maintaining the sensitivity and selectivity required for clinical applications.

3.6. Greenness, blueness, and whiteness assessment

3.6.1. AGREE greenness evaluation. The environmental impact and sustainability of the developed Rhodamine 6G-based fluorescence quenching method were comprehensively evaluated using the Analytical GREEnness Calculator (AGREE) metric tool. The AGREE assessment provides a quantitative measure of greenness based on the 12 SIGNIFICANCE principles of Green Analytical Chemistry, generating scores on a 0–1 scale where values approaching 1.0 indicate superior environmental performance. The developed method achieved a high AGREE score of 0.76, demonstrating excellent compliance with green analytical chemistry principles (Fig. 6A). This score significantly exceeds the reference HPLC-UV method reported by Shah *et al.*,[10] which obtained a moderate AGREE score of 0.66 (Fig. 6B), indicating a substantial improvement in environmental sustainability.

Table 4 Statistical comparison between the developed fluorescence method and reference HPLC-UV method for pharmaceutical formulation analysis

Method	Mean[a]	SD	*t*-test (2.306)[b]	*P* Value	*F*-Value (6.338)[b]	*P* Value	θ_L[c]	θ_U[c]
Developed method	99.94	0.871	0.336	0.746	1.582	0.668	−1.233	1.653
Reported method	99.73	1.095						

[a] Average of five determinations. [b] The values in parenthesis are tabulated values of "*t* "and "*F*" at ($P = 0.05$). [c] Bias of ± 2% is acceptable.

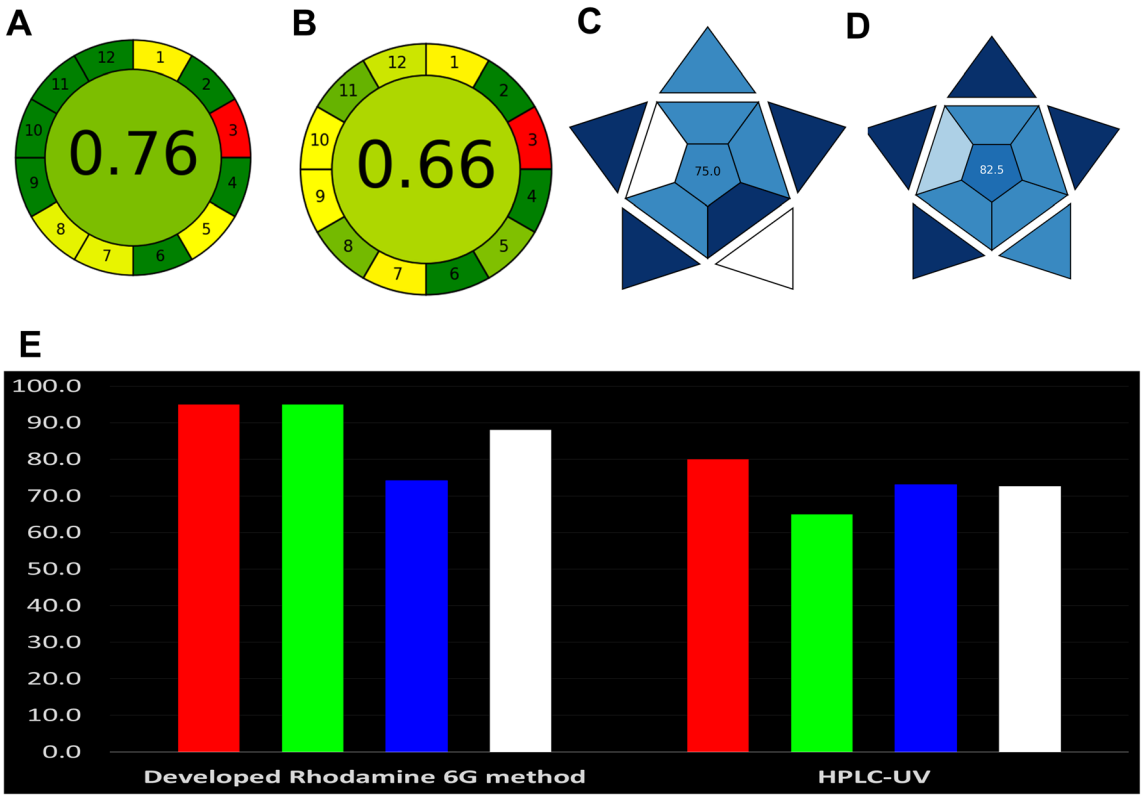

Fig. 6 Greenness, blueness, and whiteness assessment. (A) AGREE pictogram for the developed fluorescence method (score: 0.76). (B) AGREE pictogram for reference HPLC-UV method (score: 0.66). (C) BAGI asteroid plot for fluorescence method (score: 75.0). (D) BAGI asteroid plot for HPLC-UV method (score: 82.5). (E) White analytical chemistry assessment showing RGB components and overall whiteness scores.

Detailed analysis revealed the fluorescence-based approach demonstrated significant environmental advantages across multiple green chemistry principles. For example, principle 7 (waste generation) showed superior performance for the developed method, generating minimal aqueous waste. This contrasts favorably with HPLC mobile phase consumption, requiring organic waste disposal protocols. Similarly, principle 9 (energy consumption) clearly favored the fluorescence approach due to substantially lower power requirements of fluorescence spectrophotometers compared to HPLC systems requiring high-pressure pumps and extended operation times. Additionally, principle 12 (operator safety) showed significant improvement through elimination of organic solvent exposure and high-pressure systems while operating with benign aqueous reagents at ambient conditions. However, certain limitations were identified in the fluorescence approach. For example, principle 5 (automation and miniaturization) favored the HPLC-UV method due to automated injection and sample handling capabilities of modern autosamplers, whereas the fluorescence method currently requires manual sample preparation and measurement steps. Despite this limitation, the systematic improvements across waste generation, energy consumption, reagent sourcing, and operator safety collectively validate the environmental superiority of spectrofluorimetric detection for sustainable pharmaceutical analysis of mefenamic acid.

3.6.2. BAGI practicality assessment. The practical applicability and user-friendliness of the analytical methods were evaluated using the Blue Applicability Grade Index (BAGI), which assesses ten key attributes related to method practicality, operational simplicity, and real-world implementation feasibility. The BAGI evaluation provides scores ranging from 25–100, with methods achieving ≥60 points considered practically viable for routine analytical applications. The developed Rhodamine 6G method achieved a BAGI score of 75.0 (Fig. 6C), indicating good practical applicability and confirming its suitability for routine pharmaceutical applications. The reference HPLC-UV method demonstrated superior practicality with a BAGI score of 82.5 (Fig. 6D), reflecting the established analytical infrastructure and widespread familiarity with chromatographic techniques.

Analysis of the BAGI asteroid pictograms revealed distinct practical performance patterns. The developed fluorescence method demonstrated excellent performance in several attributes, showing dark blue segments for reagent availability, sample amount requirements, and preconcentration needs. The method achieved good scores (blue segments) for analytical technique accessibility and sample preparation simplicity, benefiting from straightforward aqueous solution handling and minimal sample volumes. However, significant limitations were evident in multi-analyte capability and automation degree, where white segments indicated substantial practical

challenges. The fluorescence method's inherent selectivity constraints limit simultaneous determination of multiple analytes, while manual sample preparation and measurement steps reduce automation potential compared to modern HPLC autosamplers.

Conversely, the HPLC-UV method exhibited more balanced practical performance with predominantly blue and light blue segments, indicating consistent moderate-to-good scores across most attributes. The BAGI assessment confirms that while both methods achieve practical viability above the 60-point threshold, the choice between approaches depends on specific laboratory requirements, with fluorescence offering simplicity advantages and HPLC providing comprehensive analytical capabilities.

3.6.3. White analytical chemistry and sustainability integration. The holistic evaluation of analytical method sustainability was conducted using White Analytical Chemistry (WAC) principles, which integrate analytical efficiency (red), environmental impact (green), and practical considerations (blue) into a comprehensive assessment framework. The WAC approach, based on the RGB color model, provides a balanced perspective on method sustainability by avoiding the prioritization of any single criterion while ensuring adequate performance across all essential attributes. The whiteness parameter, calculated as the average of red, green, and blue components, serves as an overall measure of method sustainability and fitness-for-purpose.

The developed Rhodamine 6G method achieved high performance across the WAC evaluation, demonstrating outstanding red (analytical efficiency) and green (environmental) scores of 95.0% each, coupled with a good blue (practical) score of 74.2%, resulting in an overall whiteness of 88.1% (Fig. 6E). This superior whiteness value significantly exceeds the reference HPLC-UV method, which achieved moderate scores of red (80.0%), green (65.0%), and blue (73.1%), yielding a whiteness of 72.7%. The 21% improvement in overall sustainability demonstrates the substantial advantages of the fluorescence-based approach when evaluated holistically.

The Red component assessment revealed superior analytical efficiency for the developed method, reflecting excellent sensitivity (LOD: 29.2 ng mL^{-1}), precision (RSD < 2%), accuracy (98.48% recovery), and broad scope of application across pharmaceutical and biological matrices. The high green component score confirmed the environmental superiority established through AGREE assessment, emphasizing minimal reagent consumption, reduced waste generation, and lower energy requirements. The blue component, while achieving good performance, identified areas for potential enhancement, particularly in automation integration and multi-analyte capabilities in agreement with the BAGI results.

Comparative analysis revealed that conventional HPLC-UV methods, despite their established analytical performenc, suffer from significant environmental drawbacks that compromise overall sustainability. The moderate green score for HPLC-UV primarily resulted from substantial organic solvent consumption, higher energy requirements, and increased waste generation characteristic of chromatographic separations. Furthermore, the extended analysis times and complex mobile phase preparations negatively impacted both environmental and practical assessments.

The WAC evaluation conclusively demonstrates that the developed Rhodamine 6G-based fluorescence quenching method represents a significant advancement toward sustainable analytical chemistry. By achieving superior performance in critical sustainability metrics while maintaining analytical excellence, this approach exemplifies the successful integration of green analytical chemistry principles with practical analytical requirements. The method's high whiteness value positions it as an optimal choice for laboratories seeking to implement environmentally responsible analytical practices without compromising analytical quality or operational efficiency. This comprehensive sustainability assessment validates the method's potential for widespread adoption in pharmaceutical quality control and therapeutic drug monitoring applications, contributing to the broader goals of sustainable development in analytical chemistry.

3.7. Comparison with reported literature

The developed Rhodamine 6G-based fluorescence quenching method demonstrates superior analytical performance compared to existing techniques for mefenamic acid determination across multiple critical parameters. Among chromatographic approaches, conventional HPLC-UV methods show significant limitations in sensitivity and analysis time. The stability-indicating method by Shah *et al.* achieved a detection limit of 10 μg mL^{-1} with rapid analysis (3.98 min retention time, 7 min run time) but remains insufficient for bioanalytical applications requiring sub-microgram detection.[10] The method by Dhumal *et al.* demonstrated improved sensitivity (0.5–2 μg mL^{-1} linearity) but suffered from prolonged analysis time with 18.253 min retention time, severely limiting analytical throughput.[11] The HPLC method by Al-Qaim *et al.* provided moderate performance (0.5–250 mg L^{-1} linearity, 3.9 min retention time),[12] while the bioanalytical HPLC-UV approach by Uddin *et al.* achieved better sensitivity for plasma analysis (250–5000 ng mL^{-1}, LOD: 70 ng mL^{-1}) with 5.4 min retention time.[13] Advanced LC-MS/MS methodology by Mahadik *et al.* demonstrated exceptional sensitivity (20–6000 ng mL^{-1}, LLOQ: 20 ng mL^{-1}) with ultra-rapid analysis (0.85 min retention time, 1.75 min run time) but requires substantial investment and specialized expertise.[14] The developed method achieves comparable sensitivity (LOD: 29.2 ng mL^{-1}) while maintaining operational simplicity and cost-effectiveness.

Alternative analytical approaches reveal various limitations that the developed method successfully addresses. Electrochemical methods show promise for sensitive detection, with Alagarsamy *et al.* achieving high sensitivity (LOD: 0.0079 μM) using modified glassy carbon electrodes,[15] while Naeemy *et al.* demonstrated simultaneous determination capabilities with paracetamol (LOD: 24–30 ng mL^{-1}) using graphene-modified electrodes.[16] However, these approaches suffer from electrode preparation complexity, matrix fouling susceptibility, and limited electrode lifetime in biological samples. Existing spectrofluorimetric methods demonstrate significant spectral

disadvantages compared to the developed approach. The aluminum(III) complexation method by Albero *et al.* achieved moderate sensitivity (0.30–16.1 μg mL^{-1} linearity, LOQ: 0.18 μg mL^{-1}) but operates at 454 nm emission where biological matrices exhibit substantial autofluorescence interference.[24] The cerium(IV) oxidation approach by Tabrizi showed acceptable sensitivity (0.03–1.5 mg L^{-1}, LOD: 0.009 mg L^{-1}) but requires toxic cerium reagents and operates in the UV region (354 nm emission) with significant matrix interference potential.[25]

The most recent spectrofluorimetric development by El Azab *et al.* using *N*-phenyl-1-naphthylamine achieved improved sensitivity (0.50–9.00 μg mL^{-1}, LOD: 60.00 ng mL^{-1}).[26] However, this approach still operates at 480 nm emission causing blue region interference and provides 2-fold lower sensitivity compared to the developed method. The Rhodamine 6G-based approach achieves superior detection sensitivity (29.2 ng mL^{-1}) while operating at optimal emission wavelength (555 nm) that effectively eliminates biological matrix autofluorescence problems encountered by existing fluorescence methods. The combination of high sensitivity comparable to advanced chromatographic techniques, freedom from matrix interference, environmental sustainability (AGREE score: 0.76, whiteness: 88.1%), and cost-effectiveness establishes the developed method as a comprehensive solution for routine mefenamic acid determination. The method provides adequate linear range (0.1–4.0 μg mL^{-1}) covering both pharmaceutical quality control and bioanalytical applications while maintaining excellent precision and accuracy, representing a significant advancement in sustainable pharmaceutical analysis.

4. Conclusion

This study successfully developed and validated a novel, sensitive, and environmentally sustainable spectrofluorimetric method for mefenamic acid determination using Rhodamine 6G as a fluorescent probe. Mechanistic studies revealed static quenching with Stern–Volmer constants of 2.43×10^5 M^{-1} at 298 K, confirming thermodynamically favorable binding through exothermic interactions ($\Delta H = -13.87$ kJ mol^{-1}) and positive entropy changes ($\Delta S = 60.81$ J (mol^{-1} K^{-1})). Central composite design optimization through rotatable design methodology established optimal experimental conditions yielding 76.4% quenching efficiency with excellent model reliability ($R^2 = 0.9897$, adequate precision = 35.58). Complete ICH validation confirmed high analytical performance including linear response over 0.1–4.0 μg mL^{-1} concentration range, superior sensitivity with 29.2 ng mL^{-1} detection limit and 96.4 ng mL^{-1} quantification limit, high accuracy of 98.48 ± 1.47% recovery, and precision parameters below 1.89% RSD for both intra-day and inter-day measurements. The method achieved statistical equivalence with reference HPLC approaches for pharmaceutical analysis and excellent biological sample recovery ranging from 96.30% to 102.21% across therapeutic concentration levels. Comprehensive sustainability assessment revealed significant environmental advantages with AGREE scores of 0.76 *versus* 0.66 for conventional methods and superior whiteness values of 88.1% compared to 72.7% for chromatographic approaches. The developed method represents a viable green analytical alternative that combines analytical excellence with environmental sustainability for routine mefenamic acid determination in pharmaceutical quality control and therapeutic monitoring.

Conflicts of interest

There are no conflicts of interest to declare.

Data availability

The authors confirm that the data supporting the findings of this study are available within the article and its SI file. See DOI: https://doi.org/10.1039/d5ra05667e.

Acknowledgements

This work was supported and funded by the Deanship of Scientific Research at Imam Mohammad Ibn Saud Islamic University (IMSIU) (grant number IMSIU-DDRSP2501).

References

1 A. Tsoupras, D. A. Gkika, I. Siadimas, I. Christodoulopoulos, P. Efthymiopoulos and G. Z. Kyzas, *Pharmaceuticals*, 2024, **17**, 627.
2 B. S. Williams, in *Essentials of Pain Medicine*, Elsevier, 2018, pp. 457–468.
3 H. Mustafa, S. Daud, S. Sheraz, M. Bibi, T. Ahmad, A. Sardar, T. Fazal, A. Khan and O. U. R. Abid, *Arch. Pharmazie*, 2025, **358**, e70004.
4 J. K. Gierse, S. D. Hauser, D. P. Creely, C. Koboldt, S. H. Rangwala, P. C. Isakson and K. Seibert, *Biochem. J.*, 1995, **305**, 479–484.
5 C. Klose, I. Straub, M. Riehle, F. Ranta, D. Krautwurst, S. Ullrich, W. Meyerhof and C. Harteneck, *Br. J. Pharmacol.*, 2011, **162**, 1757–1769.
6 J. Marjoribanks, R. O. Ayeleke, C. Farquhar, M. Proctor, C. Gynaecology and F. Group, *Cochrane Database Syst. Rev.*, 1996, 2015.
7 J. Bonnar and B. L. Sheppard, *BMJ*, 1996, **313**, 579–582.
8 H. D. C. Nierenburg, J. Ailani, M. Malloy, S. Siavoshi, N. N. Hu and N. Yusuf, *Headache J. Head Face Pain*, 2015, **55**, 1052–1071.
9 N. Cimolai, *Expet Rev. Clin. Pharmacol.*, 2013, **6**, 289–305.
10 S. N. Shah, A. Z. Mirza, H. Shamshad, N. Shafi and M. A. Naz, *Med. Chem. Res.*, 2012, **21**, 3591–3597.
11 B. R. Dhumal, K. P. Bhusari, M. R. Tajne, M. H. Ghante and N. S. Jain, *J. Appl. Pharmaceut. Sci.*, 2014, **4**, 060–064.
12 F. F. Al-Qaim, M. Abdullah, M. R. Othman and W. Khalik, *Int. J. Chem. Sci.*, 2014, **12**, 62–72.
13 A. Uddin, H. J. Mohamad, M. Al-aama and N. Amiruddin, *Int. J. Pharm. Pharmaceut. Sci.*, 2014, **6**, 167–170.
14 M. Mahadik, S. Dhaneshwar and R. Bhavsar, *Biomed. Chromatogr.*, 2012, **26**, 1137–1142.

15 S. Alagarsamy, V. Mariyappan, S.-M. Chen, R. sundaresan, T.-W. Chen, T.-W. Tseng, S.-P. Rwei and J. Yu, *Int. J. Electrochem. Sci.*, 2022, **17**, 220643.
16 A. Naeemy, R. Gholam-Shahbazi and A. Mohammadi, *J. Electrochem. Sci. Technol.*, 2017, **8**, 282–293.
17 A. Serag, R. M. Alnemari, M. H. Abduljabbar, M. E. Alosaimi and A. H. Almalki, *Spectrochim. Acta, Part A*, 2024, **315**, 124245.
18 A. H. Almalki, A. H. Abdelazim, M. E. Alosaimi, M. H. Abduljabbar, R. M. Alnemari, A. K. Bamaga and A. Serag, *RSC Adv.*, 2024, **14**, 4089–4096.
19 M. E. Alosaimi, A. H. Almalki, M. H. Abduljabbar, R. M. Alnemari, S. I. Alaqel and A. Serag, *Luminescence*, 2024, **39**, e70060.
20 R. A. Felemban, M. H. Abduljabbar, R. M. Alnemari, R. M. Alzhrani, Y. S. Althobaiti, M. F. Aldawsari, A. Serag and A. H. Almalki, *RSC Adv.*, 2025, **15**, 8855–8866.
21 S. F. Miski, A. Serag, A. S. Alqahtani, M. H. Abduljabbar, R. M. Alnemari, R. M. Alzhrani and A. H. Almalki, *RSC Adv.*, 2025, **15**, 23124–23135.
22 A. S. Alqahtani, F. M. Almutairi, M. M. Aldhafeeri, Y. S. Althobaiti, M. H. Abduljabbar, A. Serag and A. H. Almalki, *Spectrochim. Acta, Part A*, 2025, **327**, 125342.
23 R. M. Alnemari, M. H. Abduljabbar, Y. S. Althobaiti, S. Alshehri, F. M. Almutairi, H. A. Shmrany, E. S. Alatwi, A. Serag and A. H. Almalki, *J. Photochem. Photobiol., A*, 2025, **465**, 116357.
24 M. I. Albero, C. Sanchez-Pedreño and M. S. Garcia, *J. Pharm. Biomed. Anal.*, 1995, **13**, 1113–1117.
25 A. B. Tabrizi, *Bull. Korean Chem. Soc.*, 2006, **27**, 1199–1202.
26 N. F. El Azab, S. M. Alqirsh, N. Magdy and M. F. Abdel-Ghany, *Luminescence*, 2024, **39**, e4819.
27 S. Zeng, X. Liu, Y. S. Kafuti, H. Kim, J. Wang, X. Peng, H. Li and J. Yoon, *Chem. Soc. Rev.*, 2023, **52**, 5607–5651.
28 D. Magde, R. Wong and P. G. Seybold, *Photochem. Photobiol.*, 2002, **75**, 327–334.
29 M. Y. Dhamra and N. Theia'a, *Pak. J. Anal. Environ. Chem.*, 2021, **22**, 367–375.
30 F. Pena-Pereira, W. Wojnowski and M. Tobiszewski, *Anal. Chem.*, 2020, **92**, 10076–10082.
31 N. Manousi, W. Wojnowski, J. Płotka-Wasylka and V. Samanidou, *Green Chem.*, 2023, **25**, 7598–7604.
32 P. M. Nowak, R. Wietecha-Posłuszny and J. Pawliszyn, *TrAC, Trends Anal. Chem.*, 2021, **138**, 116223.
33 A. Penzkofer, A. Tyagi, E. Slyusareva and A. Sizykh, *Chem. Phys.*, 2010, **378**, 58–65.
34 M. Enoki and R. Katoh, *Photochem. Photobiol. Sci.*, 2018, **17**, 793–799.
35 J. Mandal, P. Ghorai, K. Pal, T. Bhaumik, P. Karmakar and A. Saha, *ACS Omega*, 2020, **5**, 145–157.
36 M. A. E. Hamd, B. S. Al-Farhan, S. F. Saleh, W. A. Mahdi, S. Alshehri, B. R. Alsehli and A. A. Hamad, *Talanta Open*, 2025, **11**, 100452.
37 A. Serag, F. M. Almutairi, M. M. Aldhafeeri, R. M. Alzhrani, M. H. Abduljabbar, R. M. Alnemari, Y. S. Althobaiti and A. H. Almalki, *RSC Adv.*, 2025, **15**, 19468–19479.
38 ICH, *I.C.H. Guideline*, Geneva, Switzerland, 2022, p. 1.
39 A. Serag, A. H. Abdelazim, S. Ramzy, R. M. Alnemari, R. M. Alzhrani, M. H. Abduljabbar, Y. S. Althobaiti, M. E. Alosaimi, S. I. Alaqel and A. H. Almalki, *Talanta*, 2026, **296**, 128442.
40 K. Ito, Y. Niida, J. Sato, E. Owada, K. Ito and M. Umetsu, *Pediatr. Int.*, 1994, **36**, 387–391.